Mechanisms for space applications

M. Meftah [a,*], A. Irbah [a], R. Le Letty [b], M. Barré [c], S. Pasquarella [d], M. Bokaie [e], A. Bataille [b], and G. Poiet [a]

[a] CNRS/INSU, LATMOS-IPSL, Université Versailles St-Quentin, Guyancourt, France
[b] Cedrat Technologies SA, 15 Ch. de Malacher, 38246 Meylan, France
[c] Thales Avionics Electrical Motors, 78700 Conflans Sainte-Honorine, France
[d] Vincent Associates, 803 Linden Ave., Rochester, NY 14625, United States
[e] TiNi Aerospace, 2505 Kerner Blvd., San Rafael, CA 94901, United States

ABSTRACT

All space instruments contain mechanisms or moving mechanical assemblies that must move (sliding, rolling, rotating, or spinning) and their successful operation is usually mission-critical. Generally, mechanisms are not redundant and therefore represent potential single point failure modes. Several space missions have suffered anomalies or failures due to problems in applying space mechanisms technology. Mechanisms require a specific qualification through a dedicated test campaign. This paper covers the design, development, testing, production, and in-flight experience of the PICARD/SODISM mechanisms. PICARD is a space mission dedicated to the study of the Sun. The PICARD Satellite was successfully launched, on June 15, 2010 on a DNEPR launcher from Dombarovskiy Cosmodrome, near Yasny (Russia). SODISM (SOlar Diameter Imager and Surface Mapper) is a 11 cm Ritchey-Chretien imaging telescope, taking solar images at five wavelengths. SODISM uses several mechanisms (a system to unlock the door at the entrance of the instrument, a system to open/closed the door using a stepper motor, two filters wheels using a stepper motor, and a mechanical shutter). For the fine pointing, SODISM uses three piezoelectric devices acting on the primary mirror of the telescope. The success of the mission depends on the robustness of the mechanisms used and their life.

Keywords: Mechanism, Micro-satellite, Telescope, Sun, PICARD, SODISM, Piezoelectric

1. INTRODUCTION

The use of mechanisms in space began not so long ago: about fifty years. Since then, the ability to design mechanism that can operate in space (in particular in Earth orbit) has joined with many technologies in space. If the notion of mechanism is associated with a work discipline, it is important to know that the corresponding domain is very broad. Mechanisms are systems that must be studied in terms of their structural strength, their dynamic behavior, their thermal control, their control electronics, their electromagnetic compatibility, and their tribological behavior. Therefore, their studies require multi-disciplinary knowledge. The technologies used are extremely varied and appeal to the laws of physics in several areas of expertise. When it is necessary to modify the geometry of a part of a satellite or instrument to ensure a specific function, mechanisms are used. To design a mechanism, it is necessary to have a good feedback: knowledge and experience are essential. Since the advent of the space age, many mechanisms have been used in space. It is always interesting to have a feedback on the use of a mechanism associated with a space mission. It is necessary to have a proven heritage. And it is essential to continue to establish new research to develop mechanisms for future.

SODISM is an 11 cm Ritchey-Chretien imaging telescope associated with a CCD (Charge Coupled Device), taking solar images at five wavelengths. The first image of the Sun with this new instrument was taken on July 22, 2010. Several mechanisms are used in the SODISM space instrument developed by the CNRS. SODISM uses a piezoelectrics mechanism to stabilize images of the Sun on the CCD, two filters wheels, a door at the entrance of the instrument, and a mechanical shutter.

* Corresponding author
E-mail address: Mustapha.Meftah@latmos.ipsl.fr

2. THE PICARD MISSION AND THE SODISM INSTRUMENT

The solar mission PICARD will simultaneously measure several key parameters of the Sun. The PICARD mission operate during the solar cycle 24. The scientific objectives of the PICARD mission are described in details by [1]. The orbit is chosen to allow periods of Sun visibility as long as possible. A SSO (Sun Synchronous Orbit) with an ascending node at 06h00, an altitude of 735 km (period of 99.4 minutes), and an inclination of 98 degrees was selected. The duration of eclipses will not exceed 20 minutes with these orbit parameters, in particular in December. The mission lif etime is two years; however a longer mission is expected especially given the late start of cycle 24.

PICARD (Figure 1), based on a micro-satellite platform MYRIADE from CNES (France) was launched by a DNEPR rocket on June 15, 2010. SODISM (shown in Figure 2), is one ofits on-board instruments. SODISM allows us to measure the solar diameter, the solar shape, and to perform helioseismologic observations to probe the solar interior. The instrument is described in details by [2]. This paper covers the design, development, testing, production, and in-flight expe rience of the piezoelectrics mechanism, the door, the filters wheels and the mechanical shutter.

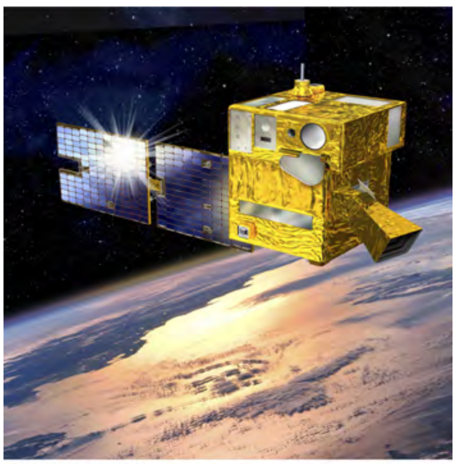

Figure 1. PICARD Satellite.

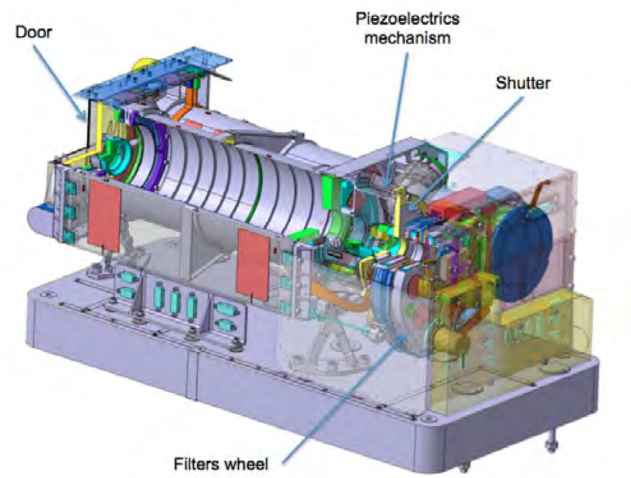

Figure 2. SODISM instrument.

3. THE PIEZOELECTRICS MECHANISM

3.1 Description of the mechanism

For the fine pointing, SODISM uses three piezoelect ric devices acting on the primary mirror M1. The piezoelectric actuator technology has been used in various instrument, notably on SOHO [3], and ROSETTA [4]. Piezoelectric actuators (Cedrat Techno logies) have been modified to get a higher mechanical preload and include piezoelectric ceramics. It is essentia l to preload such components, as they cannot bear any tensile stresses. The parallel pre-stressed actuator is a prel oaded stack oflow voltage pi ezoelectric ceramics. Piezo electric displacement is 50 µm peak for 170 V peak. The capacit ance of the piezoelectric is 2.7 µF. A tensile force test was performed to verify that the mechanical prestress is effectively app lied to the correct level. The p ower consumption depends upon the quality of the pointing. Strain gauges are used for each piezoelectric (repeatability on the positioning). For the fine pointing, SODISM uses four photodiodes (API SD9973). Any unbalanced signal between pairs of detectors indicates a modification of the pointing. Photodiodes are semiconductors that generate a current or voltage when illuminated by light. A sapphire window is used. Sapphire is a very rugged radiation resistant optical material with a very broad transmission range. In our application, there is a preamplifier with a gain of 1 Megohm. The range of SODISM pointing is between 500 nm and 600 nm. The photodiode responsivity is near 0.275 A/W (or 0.275 V/ µW) for this range of application. The stability of the photodiode responsivity is fundamental for the pointing. A lot of qualification tests have been performed to verify this stability. The photodiodes are compatible with a 2 krad total dose (200 rad per hour) at photodiodes level equivalent to LEO

(735 km) for 2-year missions. A proton test has been performed. Other tests have been performed (aging tests, burn in, thermal cycling, shocks, vibration,). The photodiode responsivity and major electrical parameters remain stable after these tests. The telescope has a mi rror M1 active actuated by three piezoelectrics to handle 2 active axes (Rx, Ry), Z being the axis of translation. Z motion can defocus the telescope. Activation of the M1 mirror helps isolating the telescope movements of the platform, via an optical sensor: that is formed by a secondary beam passing through the telescope (and therefore sensitive to the activation of M1) and sent on an electro-optical sensor (guide way). The piezoel ectric actuators are lin earized by strain gauges.

The pointing mechanism of SODISM uses piezoelectrics PPA40M-NM-SV (Figure 3). The parallel pre-stressed actuator is a preloaded stack o flow voltage piezoelectric ceramics. Th e preload (or pre-stress) is obtained from an external spring frame made of stainless steel which protects the MultiLayer Actuator (MLA) against tensile force and provides mechanical interfaces for the user allowing an easier integration. This pre-stressing frame applies an optimal preloading force to the MLA, which ensures a longer lifetime and better performance with dynamic applications than traditional preloaded actuators. Designed by the CEDRAT, this modified direct piezoelectric results from contracts carried out for CNES and CNRS. Multilayer piezoelectric component (5*5*10 mm - N17 type) is shown in Figure 4. Piezoelectric devi ces have the unique property of generating a voltage when a pressure is applied, as well as the inverse property, expanding when a voltage is applied.

When a voltage is applied to a cylindrical piezoelectric ele ment, the cylinder increases in length (and decreases in diameter). This expansion is a per cent of the total length L of the cylinder. And because the total length of a piezoelectric element is relatively small, the resulting change in total length is much smaller (in the nanometer range), which is good for applications that need high resolution across relatively short displacements. One way to increase the travel further is to stack piezoelectric eleme nts and add a leveraging system. Travel can extend to the 20, 100, or even 200 µm range. Such leveraged displacements apply less force, but they are still generally suitable for applications such as automated alignment of fibers and waveguides. For PICARD/SODISM application, we have chosen a stroke of nearly 50 µm, corresponding to angular motion of 240 arcseconds.

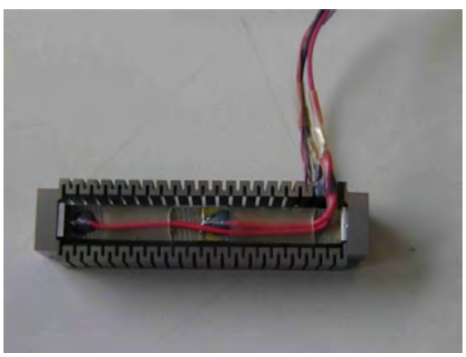

Figure 3. View of the Direct Piezoelectric.

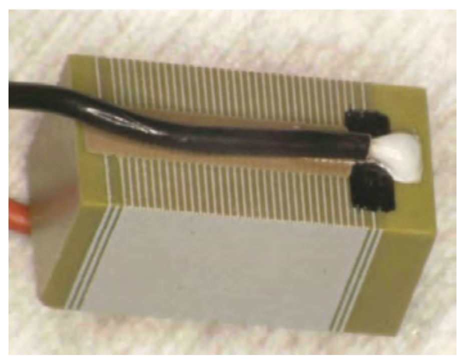

Figure 4. Standard multilayer piezoelectric component.

3.2 Pointing mechanism characteristics

The pointing mechanism is operated by global on-board electronics named the PGCU (PICARD Gestion Charge Utile). The pointing mechanism design is shown in Figure 5. A Qualification Model (QM) of the pointing mechanism is shown in Figure 6.

Table 1 summarizes the main characteristics of the mec hanism. Solar images are r ecorded every minute with SODISM and processed on-board. Every minute, the pointing mechanism is operational meaning, that the piezo actuators are driven back to 60 Volt (mean position) during 44 seconds (minimum). The Strain Gauges are continuously driven to obtain a stable thermal behavior. The fine pointing is operational two seconds before taking the picture on the CCD and the functioning of the shutter's operation (integration time between 500 ms to 16 seconds). The pointing mechanism has been built by CNRS LATMOS.

Table 1. Pointing mechanism main characteristics.

Main characteristics	Nominal values
Volume	153*141*125 mm
Weight	2.54 kg
Pointing accuracy	± 0.2 arcseconds
Offset (rotation Rx, Ry)	± 60 arcseconds
Non operating temperatures	-35 °C / +50 °C
Operating temperatures	+5 °C / +40 °C
Power consumption	2.0 W

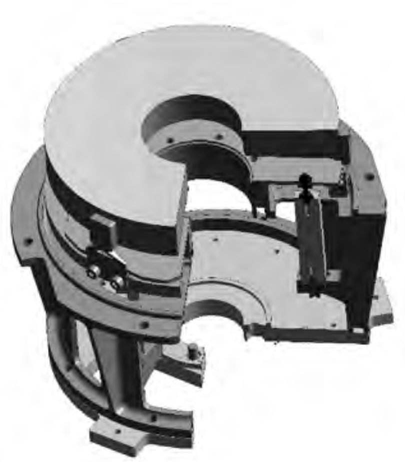

Figure 5. The pointing mechanism.

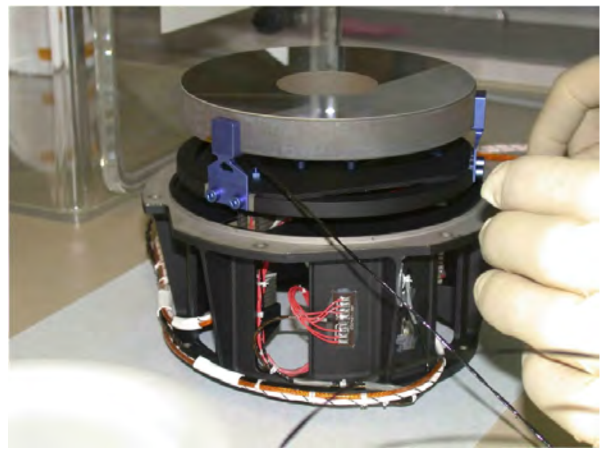

Figure 6. Qualification Model of the Pointing mechanism.

3.3 Qualification of the mechanism

3.3.1 The piezoelectric qualification

The properties defined in the Table 2, are set up according to the technical conditions of use and measurement. These properties are warranted within their variation range and in compliance with the standard technical conditions of use.

Table 2. Technical conditions of use and main measurements.

Main characteristics	Nominal values
External force maximum traction (non operating)	800 N
External force maximum compression (non operating)	1600 N
Non operating temperatures	-40°C / +50 °C
Operating temperatures	-20°C / +30 °C
Operating temperature s with performances	+10 °C / +30 °C
Displacement (voltage between -20V to 150V)	48.5 µm
Blocked force (at 150V)	950 N
Pre-Stress (Operating temperatures)	35 MPa ± 2.1
Pre-Stress (Non operating temperatures)	32.3 at 38.7 MPa
Minimum stress in the ceramic (compression)	4.5 MPa
Maximum stress in the ceramic (compression)	95 MPa
Maximum stress for the spring	630 MPa
Volume	48*12*10 mm
Weight	17.1 g

A dedicated program has been used to qualify the components, and is described in Figure 7. A Lot Acceptance Tests (LAT) was followed and includes: a Destructive Physical Analysis (DPA) (and comparison with previous results) of the piezoelectric multilayer components to be used in the program PICARD/SODISM, a tensile force test and the DPA resulting from the encountered anomaly.
As an applicable ESCC standard document does not yet exist, the standard applicable for multilayer capacitors was used to derive an appropriate qualification program. The piezoelectric components are divided into 4 groups:
- Control group: stroke, blocked force, electrical characteristics and a DPA,
- Electrical tests group: functional test under UHV (Ultra-High Vacuum), Paschen effect, electrical strength,
- Mechanical tests group: thermal shocks, fatigue, traction/compression strength,
- Humidity tests groups: this represents a life test under humid environment (40% Rh, 60% Rh and 85% Rh), which is the most critical environment for piezoelectric in use.

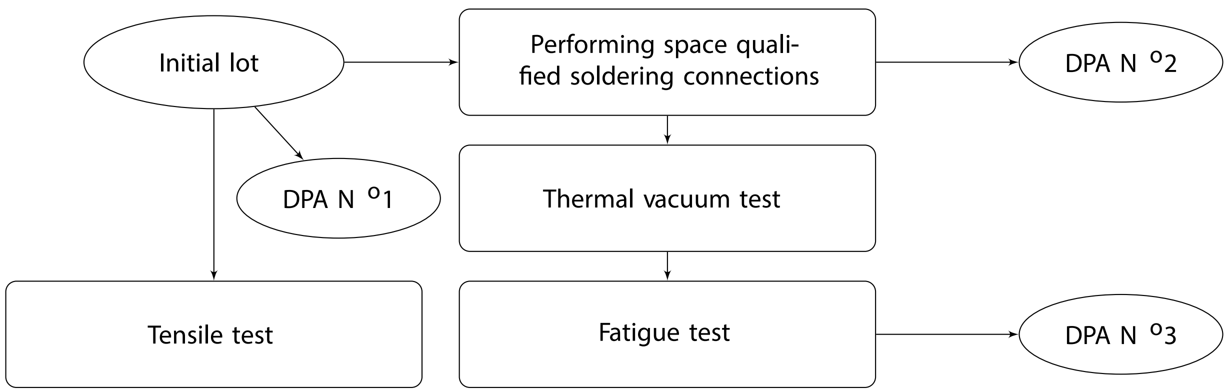

Figure 7. LAT test flow.

The main conclusion is that one piezoelectric passes the evaluation without any failure and the other one passes all the tests but not the high humidity level life test (85% Rh). This last result implies user guidelines during AIT (Assembling, Integration and Tests) operations. The influence on performance and reliability of the use of cleaning solvent was also evaluated. Part of the piezoelectric qualification was done during this campaign. Other aspects of qualification have been validated by PICARD project.

The 2 sources of piezoelectric ceramics tested are preferred components for CNES applications. One of these sources is used on the Picard satellite telescope. More recently, the application of the Reduction Of Hazardous Substances (Rohs) on piezoelectric component has lead to problems. The piezoelectric material itself often contains lead oxides that are exempted from this directive. However, the soldering connections are concerned: non-lead soldering connections are more difficult, due to a higher temperature. The Figure 8 shows an example of a non lead soldering connection of bad quality that is also responsible for a crack occurrence. The aerospace industry requires such destructive Physical Analysis to be performed for each production lot, to monitor the quality assurance product. As a consequence, all the soldering (both for the piezo and the strain gauges) connections are performed and controlled at Cedrat Technologies (Figure 9).

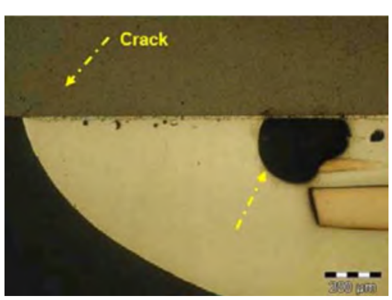

Figure 8. Cut of view of a soldering connection.

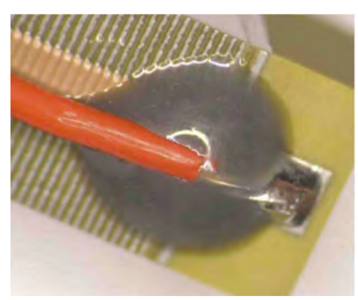
Figure 9. View of a soldering and secured connection.

The tested lot of 28 components of the N17 component was divided into 4 groups and the evaluation test program was completed according to the test plan. No fa ilure has been encountered, despite relatively long humidity resistance tests. The realized fatigue test included the following set of cycles (Table 3).

Table 3. Outcome of the functional tests before (a) and after (b) the fatigue tests.

Reference	Cycles	Displacement		Resonance	
PPA20M 06-009	4.10^{6}	23.48 µm(a)	23.21 µm(b)	39484 Hz(a)	39902 Hz(b)
PPA20M 06-010	20.10^{6}	22.64 µm(a)	22.63 µm(b)	38876 Hz(a)	39142 Hz(b)

3.3.2 The mechanism qualification

The mechanism has been qualified through a dedicated test campaign. Environments for the qualification and acceptance of the mechanism are: Ariane sine, DNEPR random, shock (Solar array r elease with pyrosofts nuts and separation of the satellite with pyro devices), thermal environment at 735 km and functional tests.

- Mechanical environment

The mechanism was designed to withstand the launch loads. Random levels are displayed in the Table 4 and have been successfully tested (Figure 10). Those levels were defined after a mechanical analysis of the coupling between the SODISM instrument and the pointing mechanism. The design was assessed by using a Finite Element Model of the pointing mechanism. It was checked through the Finite Element model that the piezo components still display a positive stress level, and that all parts display a stress budget with a minimum of 25% margin for the yield stress. The qualification vibration t est is to be run in accordance with the details given in Table 4. The mechanism is unpowered during vibration. Table 4 show the Power Spectral Density (PSD) of the acceleration injected at the i nterface of the mechanism.

Table 4. Random vibration workmanship qualification test levels (duration of 120 seconds in each of three axes).

X axis		Y axis		Z axis	
fin Hz	PSD g^2/Hz	fin Hz	PSD g^2/Hz	fin Hz	PSD g^2/Hz
20	0.1	20	0.1	20	0.1
100	2	100	1	30	3
200	2	200	1	160	3
450	0.05	400	0.05	200	0.3
1000	0.05	1000	0.05	350	0.3
2000	0.001	2000	0.001	450	0.04
–	–	–	–	1000	0.04
–	–	–	–	2000	0.005
20.3 g rms		15.3 g rms		23.4 g rms	

- Shock test

A shock test was achieved on MST Satellite (Mechanical and Thermal Structure of the Satellite) for a solar array release with pyrotechnics nuts and separation of the microsatellite with pyrotechnics devices. This test allowed qualifying the instrument SODISM with the pointing mechanism.

- Thermal environment

The thermal environment was established within the following thermal environment: between -35 ^{o}C and +50 ^{o}C (non operational). For operational conditions, the pointing mechanism thermal cycling was between +5 ^{o}C and +40 ^{o}C. 8 Thermal-vacuum cycles have been performed.

- Functional test at instrument level

To obtain a on-ground validation of the closed loop implemented in the mechanism, a dedicated test bench simulating the change of the sun position has been used (Figure 11). The characteristics of each piezo actuator (used on the flight model of the mechanism) were measured (Table 5 show main characteristics).

Table 5. Maximum measured displacement.

Reference	Displacement vs. Input voltage
Piezoelectric PPA40M N°1	50.04 µm peak-peak for 170 V peak-peak
Piezoelectric PPA40M N°2	50.39 µm peak-peak for 170 V peak-peak
Piezoelectric PPA40M N°3	50.84 µm peak-peak for 170 V peak-peak

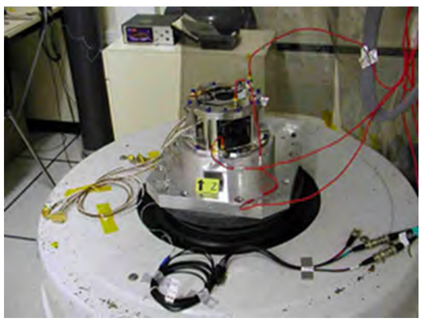

Figure 10. View of the Pointing Mechanism on the shaker.

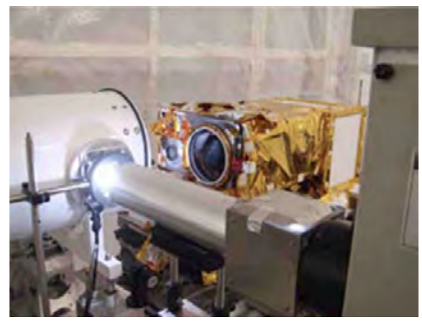

Figure 11. Test bench of SODISM instrument.

3.4 The flight performances

The Figure 12 (left side) shows the improvement brought by the pointing mechanism and its effect on the achieved image stability. An image is taken every 2 minutes, leading to 720 images per day. The Figure 12 (right side) shows the displacement of the image on the CCD performed by the pointing mechanism over 3 days. The standard deviation is equal to 0.31 pixel (whose size corresponds to 1.06 arcsecond). This means that the image stability (standard deviation) corresponds to an angular value of ± 0.234 arcsecond.

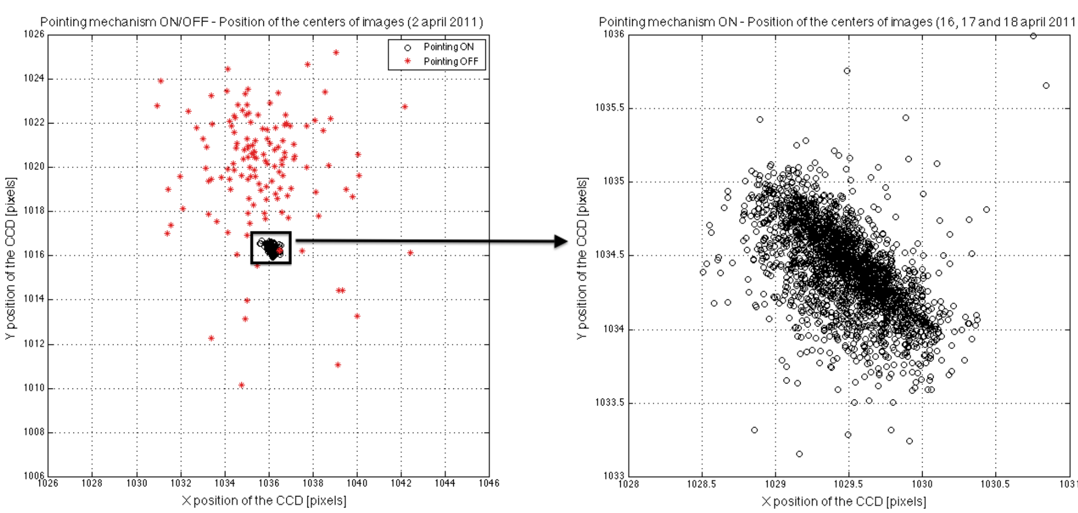

Figure 12. Pointing mechanism - ON/OFF.

4. THE FILTERS WHEEL MECHANISM

4.1 Description of the mechanism

The filters wheel (Figure 13) has 5 positions: 4 imaging filters. Each filters wheel consists of: a stepper motor size 11 from THALES AEM (formerly SFMI) with a stainless steel output pinion, a gear wheel with vespel SP3 material, a gear train with a reduction ratio 11:240, a pair of ball bearings preloaded WX9ZZT4DOK3682 from ADR, a proximity electronics board and three couples of emitters and receptors infrared Micropac 62005 and 61055 integrate on electronic board. Molybdenum disulfide (MoS_2) is the material used as solid lubricant on the ball bearings of the wheel. In the form of dry powder these materials are effective lubricant additives due to their lamellar structure. The lamellas orient parallel to the surface in the direction of motion. The friction torque of ball bearings is less than 10 g.cm.

Thales AEM designs and manufactures stepper motors and stepper gear-motors for optical space applications for over 40 years. The stepper motors are available in NEMA (National Electrical Manufacturers Association) sizes 08, 11 and 15 with a wide range of configurations of windings and length. In the family of stepper motors, the variable reluctance stepper motor is widely used for example in Picard's mission to drive the filter wheels of the SODISM instrument. The variable reluctance stepper motor consist of a rotor and stator each with a different number of teeth. As the rotor does not have a permanent magnet it spins freely, the motor has no detent torque. It is very important in the application where reversibility is needed. Variable reluctance stepper motors are electromagnetic rotary devices which convert digital pulses into mechanical rotation. The angle of rotation is directly proportional to the number of pulses and to the angular value of step (48 steps per turn is equal to 7.5 degrees per step). The speed of rotation is relative to the frequency of those pulses. Stepper motors are simple to drive in an open loop configuration and for this reason they are often used in positioning systems. In the space optical applications, grease is prohibited, we use ball bearings with retainers self-lubricating material. The pinions of gear-motors receive special treatment to operate without grease. All mechanical parts of the stepper motors are made of stainless steel. The coil windings are made with high quality enameled copper wire able to ensure a lifetime of 20,000 hours at 240°C. All the manufacturing processes are mature and perfectly controlled to ensure excellent reliability in a vacuum to 10^{-9} Torr and operating temperature from 55 °C to +70 °C (from -70°C to +85 °C in storage conditions). A view of the stepper motor size 11 is done in Figure 14. Major elements of the stepper motor are: 1. housing and stator assembly, 2. rotor, 3. ball bearings, 4. plain washers and curved spring washer , 5. retaining ring, 6. output pinion, 7. locking pin (between shaft and output gear).

The main characteristics of the stepper motor are: a mass of 130 grams, a resistance of 150 Ω, a minimum static torque of 140 g.cm and a starting torque greater than 50 g.cm (with 500 steps per second).

Figure 13. View of a filters wheel during integration.

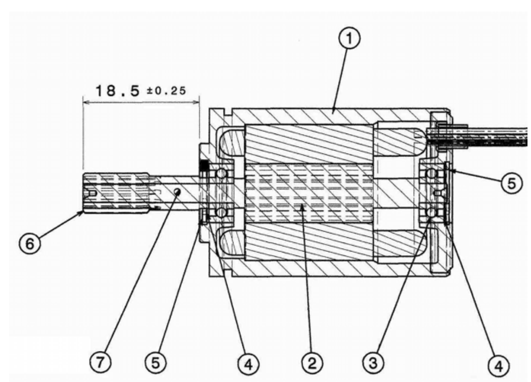

Figure 14. Stepper motor 1116112 (all dimensions in mm).

4.2 The filters wheel mechanism characteristics

Table 6 summarizes the main characteristics of the mechanism. Solar images are recorded every minute with SODISM and processed on-board. The filter wheel is operational up to 10 seconds per minute. An interference filter is positioned with a maximum accuracy of 3 motor step (1 motor step = 180 µm of displacement of the center of one filter). The filters wheel mechanism has been built by CNRS LATMOS.

Table 6. Filters wheel mechanism main characteristics.

Main characteristics	Nominal values
Volume	157*139*69 mm
Weight	0.81 kg
Positioning accuracy (Z rotation axis)	± 3 motor step
Positioning of a filter (X and Y axis)	± 8 arc-minutes
Non operating temperatures	-35 °C / +50 °C
Operating temperatures	+5 °C / +40 °C
Power consumption	7.5 W during rotation
Frequency	80 Hz (or motor step per second)

4.3 Qualification of the mechanism

The filters wheel has been tested to survive the vi bration, shock and environmental extremes.

- Mechanical environment

The mechanism was designed to withstand the launch loads. It was checked that the ball bearings have a sufficient preload of 10 N, corresponding to hertzian pressure of 824 MPa. Under this preload and the specified random vibration level, it was estimated that no gapping in the b all bearing shall occur. The l evel of hertzian pressure and the number of cycles (more than 500,000 cycles) is compatible with the selected dry lubrication (MoS2). Random levels are displayed in the Table 7 and have been successfully tested. The mechanism is unpowered during vibration.

Table 7. Random vibration workmanship qualification test levels (duration of 120 seconds in each of three axes).

X axis		Y axis		Z axis	
fin Hz	PSD g^2/Hz	fin Hz	PSD g^2/Hz	fin Hz	PSD g^2/Hz
20	0.1	20	0.1	20	0.1
100	1.5	100	1	100	2
200	1.5	200	1	160	2
2000	0.001	600	0.05	200	0.4
–	–	1000	0.05	500	0.4
–	–	2000	0.001	700	0.04
–	–	–	–	1000	0.04
–	–	–	–	2000	0.005
18.5 g rms		16.4 g rms		20.0 g rms	

- Shock test

The mechanism is unpowered during the test. The filters wheel has been qualified under high shock level by a representative test (hammer shock testing). Mechanical shock pulses are often analyzed in terms of shock response spectra. The shock response spectrum assu mes that the shock pulse is applied as a common base input to an array ofindependent single-degree-of-freedom systems. The shock response spectrum gives the peak response of each system with respect to the natural frequency. Damping is typically fixed at a constant value, such as 5%, which is equivalent to an amplification factor of Q=10. Levels of shock test (in each of three axes) are: 20 g at 100 Hz and 800 g between 1000 Hz and 10000 Hz. After each shock test, a functional test was performed on the filters wheel.

- Thermal environment

The thermal environment was established within the following thermal environment: between -35 °C and +50 °C (non operational). For operational conditions, the pointing mechanism thermal cycling was between +5 °C and +40 °C. 8 Thermal-vacuum cycles have been performed.

- Functional tests and life test

The objective offunctional tests was to demonstrate full operability and performances of the mechanism in SODISM configuration, and their compatibility with the space environment. A set offunctional tests were developed and used repeatedly to quickly check the health of the filters wheel at key points in the test campaign. The main characteristics of the filter s wheel were also verified. A life tes t program on a dedicated filters wheel was implemented. The filters wheel is a critical mechani cal and electrical element that have limited lifetimes. The system has to operate in the vacuum of 293 Kelvin during a ground-test (6 months) and also in space (up to 2 years). The filters wheel has been qualified to survive a minimum of 444,400 cycles.

4.4 The flight performances

The PICARD/SODISM filters wheels are in orbit since June 2010 and are operational. 51,892 cycles are done per year (maximum for the filters wheel 2). The evol ution of temperature of the filters wheels is shown in Figure 15.

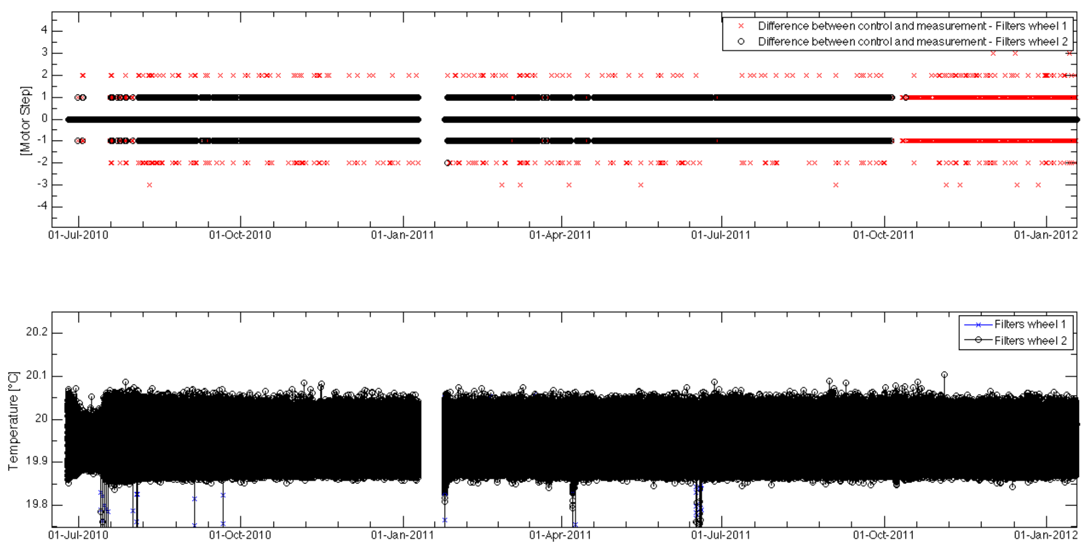

Figure 15. Evolution electronic command and temperature of filters wheels (in space).

5. THE DOOR AT THE ENTRANCE

5.1 Description of the mechanism

The door (Figure 16) has three positions: closed, partially closed and open. The door at the entrance was used to protect the instrument against contamination. The mechanism consists of: a stepper motor size 11 from THALES AEM, 5-stage epicycloidal gear-box (ratio 1166:1), two pairs of ball bearings preloaded WX9ZZT4DOK3682 from ADR, two ABB micro-switch (reference 6932) and a pin puller P25 provided by TiNi Aerospace. A view of the steppe r gear-motor size 11 is done in Figure 17. Major elements of the stepper gear-motor are: 1. stepper motor, 2. 5-stage epicycloidal gearbox (ratio 1166:1) and 3. fine thread (assembly of the flanges with the ring gear). The main characteristics of the stepper gear-motor are: a mass of 245 grams, a resistance of 150 Ω, a torque of 3000 g.cm (with 500 steps per second). The main characteristics of the pin puller are: a mass of 100 grams, a resistance of 3 Ω, a stroke of 9.5 mm and a pull force (beginning of travel) of 142 N.

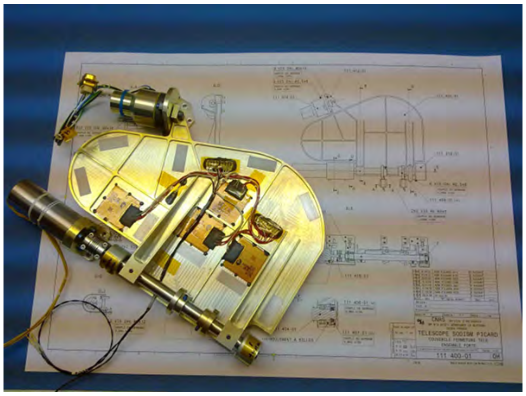

Figure 16. View of the door.

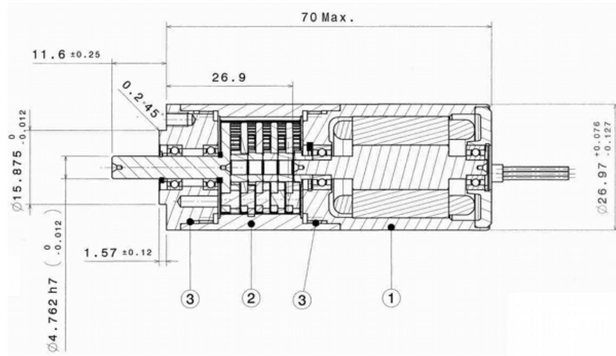

Figure 17. Stepper gear-motor 111611G1166A109.

5.2 The mechanism characteristics

Table 8 summarizes the main characteristics of the m echanism. The mechanism (stepper gear-motor) is operating twice in space (after the outgassing phase of the instrument in space and the end oflife of the satellite). The pin puller is used only one time in space.

Table 8. Door main characteristics.

Main characteristics	Nominal values
Volume	168*250*54 mm
Weight	0.98 kg
Positioning accuracy (Y rotation axis)	36 arcminutes
Non operating temperatures	-35 ^{o}C / +50 ^{o}C
Operating temperatures	+5 ^{o}C / +40 ^{o}C
Power consumption	7.5 W during rotation (58 seconds)
Frequency	500 Hz (or motor step per second)
Pin puller function time	less than 25 ms (for -40 ^{o}C and an operating current of 5A)

5.3 Qualification of the mechanism

The door at the entrance of the telescope has been tested to survive the vibration, shock and environmental extremes.

- Mechanical environment

The mechanism was designed to withstand the launch l oads. The Finite Element model was used to estimate the force acting on the pin puller (less than 1110 N), it was checked also that the pin puller demonstrates an adequate motorization margin. Ra ndom levels are displayed in the Table 9 and have been successfully tested. The mechanism is unpowered during vibration.

- Shock test

The door has been qualified under high shock level by a representative test (hammer shock testing). Levels of shock test (in each of three axes - Q=10) are: 20 g at 100 Hz and 800 g between 1000 Hz and 10000 Hz. After each shock test, a functional test was performed on the door.

- Thermal environment

The thermal environment was established within the following thermal environment: between -35 ^{o}C and +50 ^{o}C (non operational). For operational conditions, the pointing mechanism thermal cycling was between +5 ^{o}C and +40 ^{o}C. 8 Thermal-vacuum cycles have been performed.

Table 9. Random vibration workmanship qualification test levels (duration of 120 seconds in each of three axes).

X axis		Y axis		Z axis	
fin Hz	PSD g^2/Hz	fin Hz	PSD g^2/Hz	fin Hz	PSD g^2/Hz
20	0.01	20	0.01	20	0.01
100	0.1	200	0.1	100	0.1
150	1.6	250	0.3	150	0.5
200	1.6	400	0.3	200	0.5
2000	0.005	2000	0.005	2000	0.02
17.9 g rms		11.6 g rms		13.9 g rms	

- Functional tests and life test

The objective offunctional tests was to demonstrate full operability and performances of the mechanism in SODISM configuration, and their compatibility with the space environment. A set offunctional tests were developed and used repeatedly to quickly check the health of the door at key points in the test campaign. The main characteristics of the door were also verified. A life test program on a dedicated door was implemented. The door is a critical mechanical and electrical eleme nt that have limited lifetimes. The system has to operate in the vacuum during a ground-test and also in space. The door has been qualified to survive a minimum of 1,225 cycles (stepper gear-motor) and 100 cycles (pin puller).

5.4 The flight performances

The door of the instrument SODISM was successfully unlocked and opened in July 2010, during the commissioning phase. At the first use of the door in space, we encountered a problem with detecting the position of the door. We do not know the precise opening angle of the door (between 150^o and 160^o relative to the installation plan).

6. THE SHUTTER MECHANISM

6.1 Description of the mechanism

The electronic shutter (Figure 18) in operation aboard PICARD/SODISM is an electro-programmable shutter with an aperture of 35 mm (VS type), modified for this particular space flight application. The shutter allows a great deal of flexibility for mounting the shutter in a limited area (uncased version). This is especially important when design space is critical. Vincen t Associates shutters (Uniblitz) have been used in other space-borne applications in the past. VS35 type shutter was a part of the SOLSE (in 1997) and SOLSE-2 (in 2003) experiment packages aboard the Space Shuttle, and the 25mm shutters, flew to Halley's Comet aboard the Vega Probes (in 1986). Several changes were made on the nominal shutter (Figure 19). The main objective was to obtain a shutter more robust.

The main changes (PICARD/SODISM application) are described below :

- AlMgF2 (Aluminum Magnesium Fluoride) coating, reflective surface on the opposite side of blades,
- Teflon (Release) black coating used on front side of blades and on base plate,
- EAR damping system and polyethylene outer damp material (change black hard damp to white),
- Encapsulated coil with Kapton wires leads (magnet wire, polyimide varnish compatible with Kapton tape, and Hysol encapsulant black),
- Dual synchronization systems, one for each blades with Kapton lead wires with a detection of 80 % opening shutter (28 mm aperture) with receptor,
- Two couples of emitters and receptors infrared Mi cropac 62005 and 61055 integrate on electronic board,
- Heat sink installed around actuator coil (with two extremes), no heat conductive grease installed,
- Usage of Scotch Weld type two part epoxy,
- Extended legs on armature springs,
- Proper welds are provided to secure the bottom portion of the shutters guide plate.

The properties defined in the Table 10, are set up according to the technical conditions of use and measurement.

Table 10. Technical conditions of use and main measurements.

Main characteristics	Nominal values
Aperture	35 mm
Coil resistance	12 Ω
Pulse voltage to open	+70 V
Hold voltage	+7 V
Operating temperatures	0 ^{o}C / +80 ^{o}C
Maximum opening bounce	15%
Maximum closing bounce	5%
Total opening time	18 milliseconds
Transfer time on closing	12 milliseconds
Minimum exposure time	20 milliseconds
Typical exposure pulse	≥ 23 milliseconds

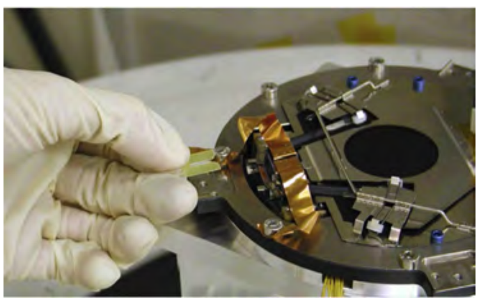

Figure 18. View of the SODISM electronic shutter.

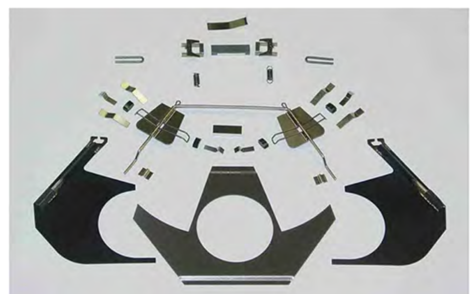

Figure 19. All elements of the shutter.

6.2 The shutter mechanism characteristics

The SODISM shutter provides exposure times between 0.5 second to 16 seconds (SODISM conditions). Table 11 summarizes the main charact eristics of the mechanism.

Table 11. Shutter mechanism main characteristics.

Main characteristics	Nominal values
Volume	108*108*15.7 mm
Weight	0.07 kg
Total opening time	≤ 30 milliseconds
Knowledge of exposure time	≤ ± 36 microseconds
Non operating temperatures	-35 ^{o}C / +50 ^{o}C
Operating temperatures	+5 ^{o}C / +40 ^{o}C
Power consumption	6.0 W during exposure time

6.3 Qualification of the mechanism

The shutter has been tested to survive environmental ex tremes to allow it to be the choice for this application.

- Mechanical environment

The mechanism was qualified to withstand the launch loads. Random levels are displayed in the Table 4 and have been successfully tested. The mechanism is unpowered during vibration.

- Shock test

The shutter has been qualified under high shock level by a representative test (hammer shock testing). Levels of shock test (in each of three axes - Q=10) are: 20 g at 100 Hz and 800 g between 1000 Hz and 10000 Hz. After each shock test, a functional test was performed on the shutter.

- Thermal environment

The thermal environment was established within the following thermal environment: between -35 ^{o}C and +50 ^{o}C (non operational). For operational conditions, the pointing mechanism thermal cycling was between +5 ^{o}C and +40 ^{o}C. 8 Thermal-vacuum cycles have been performed.

- Functional tests and life test

The objective offunctional tests was to demonstrate full operability and performances of the mechanism in SODISM configuration, and their compatibility with the space environment. A set offunctional tests were developed and used repeatedly to quickly check the health of the shutter at key points in the test campaign. The main characteristics of the shu tter were also verified. A life test program on a dedicated shutter was implemented. The shutter is a critical mechanical and el ectrical element that have limited lifetimes. The shutter has been qualified to survive a minimum of 1,329,560 exposures. Commercial Off-The-Shelf (COTS) mechanisms usually will not work for space because they will not survive the launch loads and they will stop functioning under space conditions: space is a very hostile environment. With a dedicated program, it's possible to adapt a mechanism for a use in space.

6.4 The flight performances

The PICARD/SODISM shutter is in orbit since June 2010 and is operational. 382,743 openings and closings are used per year. The evolution of total opening time and temperature of the shutter is shown in Figure 20.

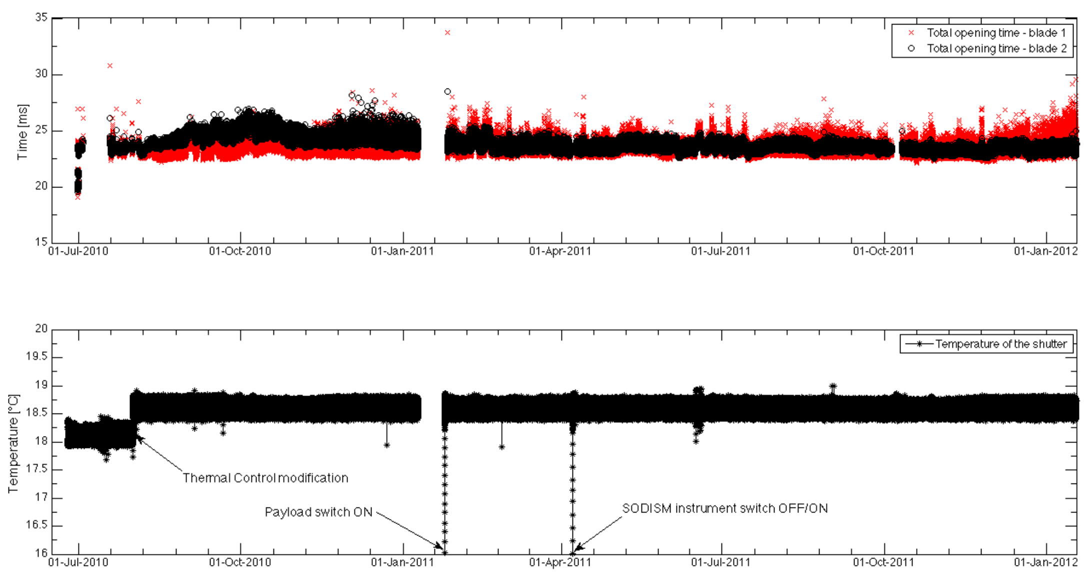

Figure 20. Evolution of total opening time and temperature of the shutter (in space).

7. CONCLUSION

An accurate pointing mechanism based on piezo actuators has been developed and qualified to compensate for the PICARD spacecraft disturbances. The flight results are in accordance with the on ground results. Such pointing mechanism is thus very effective to implement an accurate telescope on a spacecraft platform including some noises. The image stability (standard deviation) corresponds to an angular value of ± 0.23 arcsecond. With this mechanism concept, putting lots of efforts in getting a quiet platform is no longer a pre requisite ; the relative pointing error only depends on the sensor accuracy. It is envisioned to reused such approach in future missions including a telescope instrument. The piezoelectrics mechanism is in orbit since June 2010 and is operational. The PICARD/SODISM filters wheels are also operational. 51,892 cycles are done per year (maximum for the filters wheel 2). The door of the instrument SODISM was successfully unlocked and opened in July 2010, during the commissioning phase. The PICARD/SODISM shutter is in orbit since June 2010 and is operational. 382,743 openings and closings are used per year. All these mechanisms have been developed by the CNRS/LATMOS. The concepts that were used were based on industrial estates. All the mechanisms have been tested to survive the vibration, shock, and environmental extremes.

ACKNOWLEDGMENTS

We thank Cedrat Technologies SA, Thales Avionics Electrical Motors, Vincent Associates, API, ADR, TiNi Aerospace, CNES (Centre National d'Etudes Spatiales), and CNRS for their support as well as all participants having devoted their expertise to this project. PICARD development has been made possible by funding from the CNES and the CNRS. We would like to acknowledge the PICARD project teams whom are doing a remarkable work toward a successful mission.

REFERENCES

1. G. Thuillier, S. Dewitte, W. Schmutz and the PICARD team, Simultaneous Measurements of the Total Solar Irradiance and Solar Diameter by the PICARD mission, Adv. Space Res., Volume 38, Issue 8, p. 1792-1806, (2006).
2. M. Meftah, M. Meissonnier, A. Irbah et al., The space instrument SODISM and the ground instrument SODISM II, Space Telescopes and Instrumentation 2010: Optical, Infrared, and Millimeter Wave, SPIE, Vol. 7731, (2010).
3. F. Burger, J. Eder, High precision pointing device for the LASCO instrument on SOHO, 6th ESMATS proc., pp 9-14, (1995).
4. R. Le Letty et al., The scanning mechanism for ROSETTA/MIDAS from an engineering model to the flight model, 9th ESMATS proc., (2001).